MEBT-BI-EM02-03

Thermo-Mechanical Analysis of MEBT EMU/Grid

A. R. Páramo A. Vizcaíno Z. Izaola I. Bustinduy

5 July 2017

Project: MEBT
Version: 3.0
Approved by: I. Bustinduy
Revised by: Z. Izaola

Change History

Rev.	Date	Author(s)	Description
0.1	2017-04-05	A. R. Páramo	First Version
0.2	2017-04-07	A. R. Páramo	Revision
0.3	2017-07-05	A. R. Páramo	Revision. Clarification on the use of tungsten wire and its diameter..

Thermo-Mechanical Analysis of MEBT EMU/Grid

A. R. Páramo[1*], A. Vizcaino[1], , Z. Izaola[1], I. Bustinduy[1]

[1] Accelerator/Control & Diagnostics Group, ESS-Bilbao, Spain

[*]Corresponding author: arparamo@essbilbao.org

Abstract.

We study the behaviour of the EMU/Grid tungsten wire under the operational conditions expected in the ESS MEBT. From the analysis we conclude that the current design allows for safe operation, operating below thermionic emission limit of 1500 K.

1. Introduction

In this work we calculate the expected temperatures in the operational conditions for the tungsten wires used in the EMU/Grid [1, 2].

The Emittance Meter Unit (EMU), measures the beam divergence, for this purpose the EMU/Slit is installed collimating the beam with a slit aperture of 100 μm. After the EMU/Slit the beam opens, and the total aperture is measured in the EMU/Grid. The EMU/Grid is placed 400 mm downstream the EMU/Slit. Two pairs of EMU/Slits and EMU/Grids are installed, designed to measure the phase space in the horizontal and vertical directions.

In this work we study the behaviour of tungsten wires of the EMU/Grid. We study operation under the commissioning slow tuning mode [3], with beams of 62.5 mA, 3.63 MeV, 50 μs and 1 Hz. The wires have diameters of 33 μm[1]. Tungsten wires will be used due to its high secondary electron emission (compared to carbon wires), yielding a better signal [2], and due to its easier fabrication for fixing the grid wires to its frame. We assess the operational values (temperature, deformation) for the tungsten wires in the EMU/Grid. In Table 1 the main operational parameters of the EMU/Grid are summarized.

The tungsten material properties are described in Appendix A: Material Properties.

Table 1: Main parameters of the model

Paramter	Value		Parameter		Value	
Proton Energy	3.63	MeV	Slit	σ_x	3.157	mm
Intensity	62.5	mA		σ_y	3.835	mm
Irradiation Mode	50 μs - 1 Hz		Grid H.	σ_x	6.37	mm
				σ_y	0.35	mm
Wire Diameter	33	μm	Grid V.	σ_x	0.46	mm
Wire Length	76	mm		σ_y	0.35	mm
Slit – Grid Distance	400	mm				

[1] In this work the analysis is done for tungsten wires of 33 μm. The wires that will be finally installed in the EMU/Grid will have diameters of 35 μm which does not imply any major change from the design conclusions obtained in this work.

2. Model Description

2.1. Beam Size

In order to calculate the heat deposition in the EMU/Grid we assume that no optical component is activated between the EMU/Slit and EMU/Grid. Under nominal conditions we simulate, the beam size in the grid after beam collimation in the slit. We simulate the MEBT optics with TraceWin using the MEBT 2015.v0c layout.

In Table 2 and Figure 1 we show the main beam size parameters in the slit and in the grid. We refer to Slit H. for collimation with a horizontal slit, and Slit V. for collimation with a vertical slit.

Table 2: Expected Beam parameters in the EMU/Grid

Parameter		**Value**	
Slit-Grid Distance		400	mm
Slit	σ_x	3.30	mm
	$\sigma_{x'}$	6.65	mrad
	σ_y	3.98	mm
	$\sigma_{y'}$	10.08	mrad
	I_0	62.5	mA
Grid (Slit H.)	σ_x	6.37	mm
	$\sigma_{x'}$	7.12	mrad
	σ_y	0.35	mm
	$\sigma_{y'}$	0.89	mrad
	I_H^*	0.56	mA
Grid (Slit V.)	σ_x	0.46	mm
	$\sigma_{x'}$	1.165	mrad
	σ_y	0.354	mm
	$\sigma_{y'}$	10.76	mrad
	I_V^*	0.68	mA

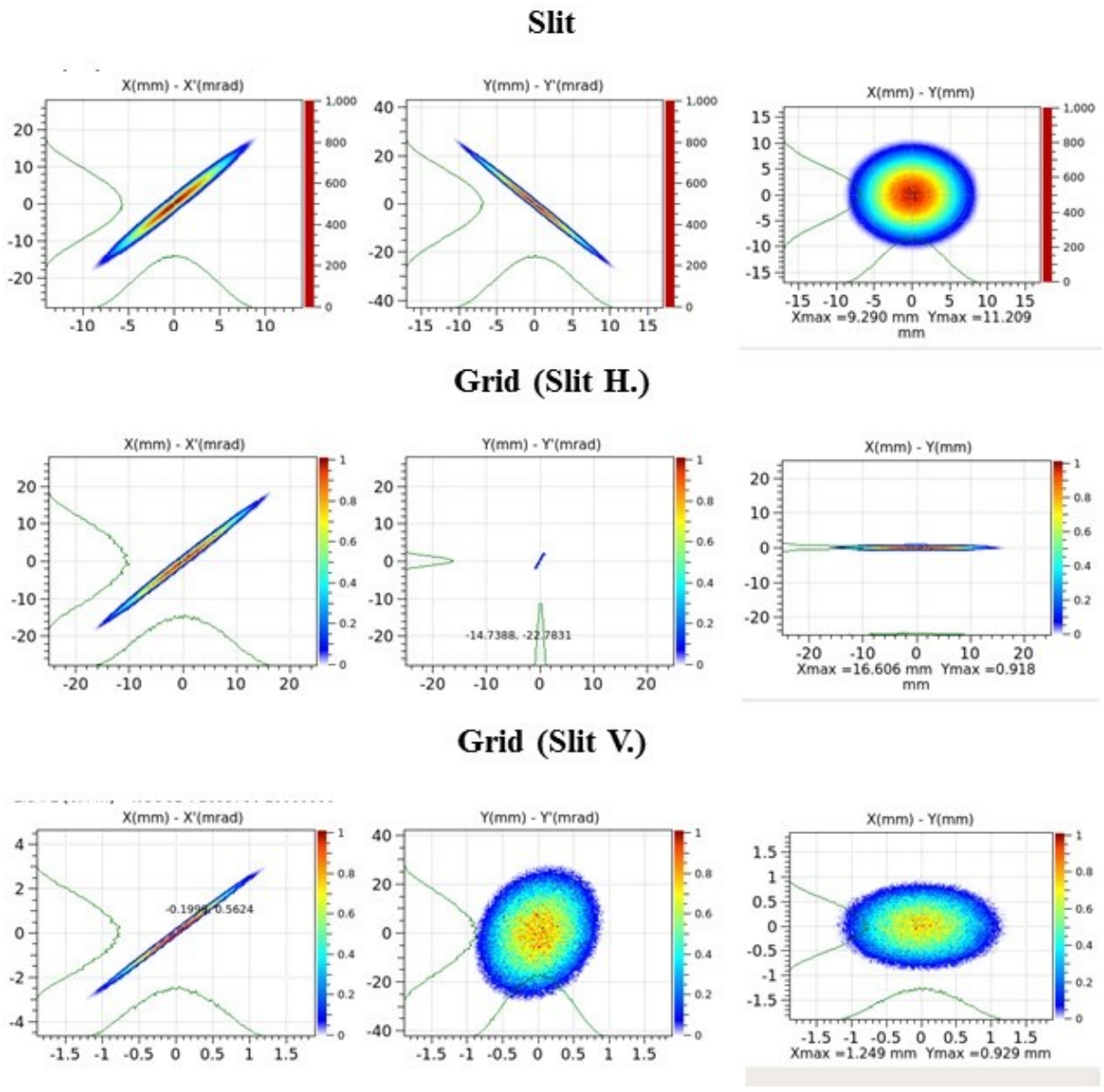

Figure 1: Beam size in the slit and in the grid for horizontal (H.) and vertical (V.) slit collimation. The figure shows the results with the MEBT 2015.v0c layout.

2.2. **Thermal Load**

The stopping power in the wire is calculated from simulations in MCNPX [4], SRIM [5] and values reported by NIST database [6].

In the case of tungsten the stopping power at the surface is ~660 MeV/cm. In Figure 2 the stopping power for tungsten is shown for MCNPX and SRIM simulations for densities of ρ=19 g/cm^3, we observe how the stopping power at the surface is ~660 MeV/cm. In the NIST data base stopping powers of ~34 MeV-cm^2/g are given, which for densities of ρ=19 g/cm^3 also means stopping powers ~660 MeV/cm.

In the case of tungsten wires of diameter larger than ~20 μm the average stopping power (S_{avg}) has to be instead of the surface stopping power due to the appearance of the Bragg Peak. The average stopping power can be estimated from the average energy deposition (E_{avg}) and the wire radius (r) as:

$$S_{avg} = E_{avg} \cdot \frac{2 \cdot r}{\pi \cdot r^2} = E_{avg} \cdot \frac{2}{\pi \cdot r} \qquad (1)$$

For tungsten wires of 33 μm diameter irradiated with 3.63 protons we have studied the irradiation using MCNPX. In Figure 3 we show the proton flux in a tungsten wire, resulting in an average energy E_{avg}=2.25 MeV for an average stopping power of S_{avg}=868 MeV/cm.

The deposited heat by a beam irradiation, $\dot{q}$, can be calculated as the multiplication of the stopping power S (MeV/cm) by the current density I'' (mA/cm^2):

$$\dot{q} = S \cdot I'' = S \cdot \frac{I_0 \cdot e^{-\left(\frac{x^2}{2\sigma_x^2}+\frac{y^2}{2\sigma_x^2}\right)}}{2 \cdot \pi \cdot \sigma_x \cdot \sigma_y} \qquad (2)$$

Where I_0 is the beam current and σ_x, σ_y the beam size.

In Figure 4 the heat deposition for the different Grid positions is shown, the maximum heat load is obtained for the vertical grids with ~60 MW/cm^3.

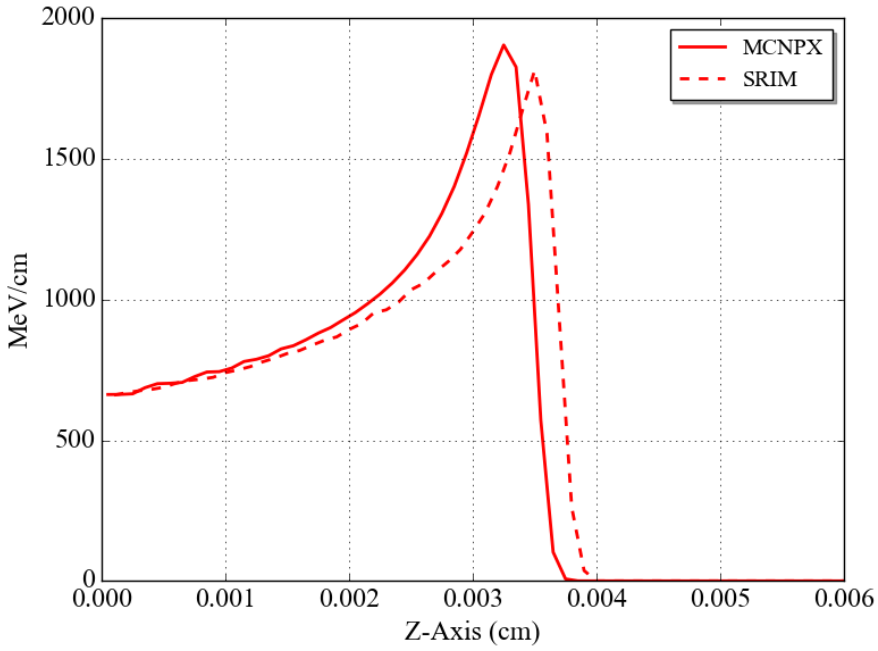

Figure 2: Stopping power for 3.63 MeV protons in tungsten, comparison of MCNPX (straight) and SRIM (dashed) models.

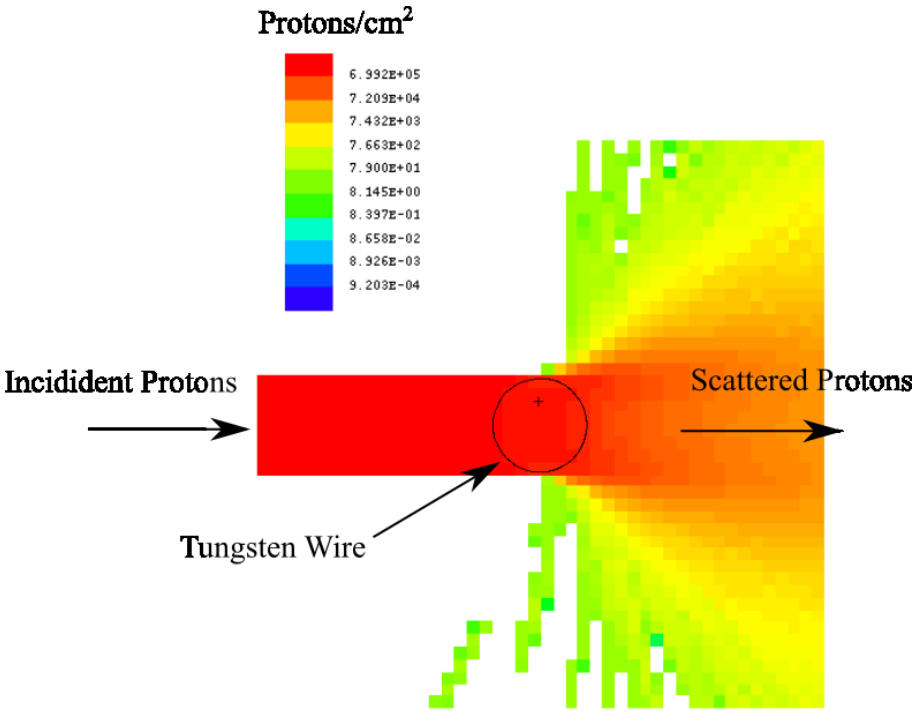

Figure 3: Protons flux of a proton beam of 3.63 MeV irradiating a tungsten wire of 33 μm of diameter.

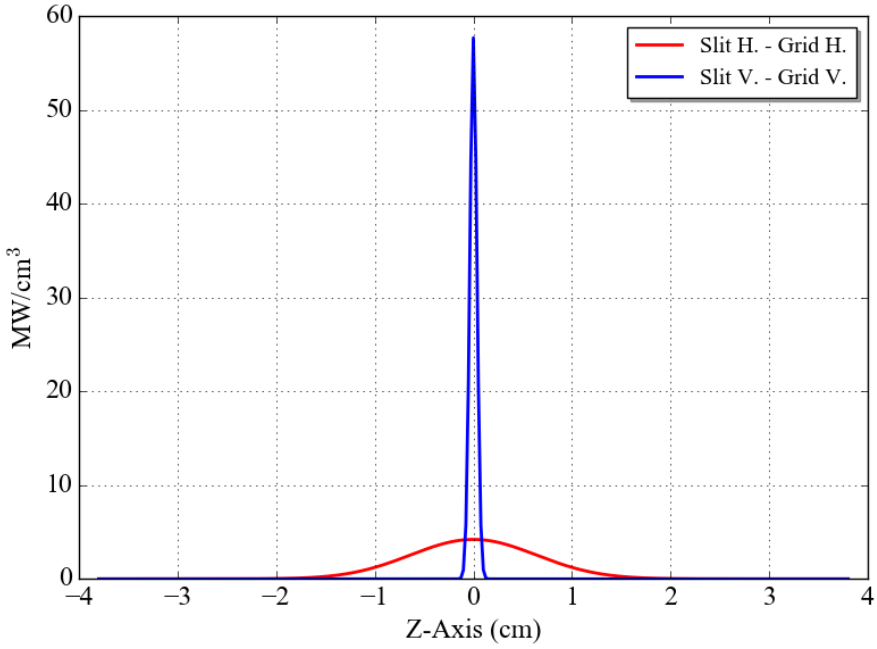

Figure 4: Heat deposition in the different Grid positions for the ESS MEBT 3.63 MeV proton beam.

2.3. **FEM Model**

In order to include thermal diffusion, an Ansys FEM model [7] is used. In the Ansys model a 1D approach is used. In the model the wire is represented by 1D beam elements and irradiation through irradiation elements to an ambient node at 300 K. Regarding the mechanical constraints, we impose them depending on the wire condition (tensile or loose). For a tensile conditions, we evaluate the stress variation assuming that wire sides are fixed. For a loose wire we calculate wire deformation in assumin free movement on one side of the wire.

In Figure 5 we show an scheme with the main components of the 1D FEM model of the wires.

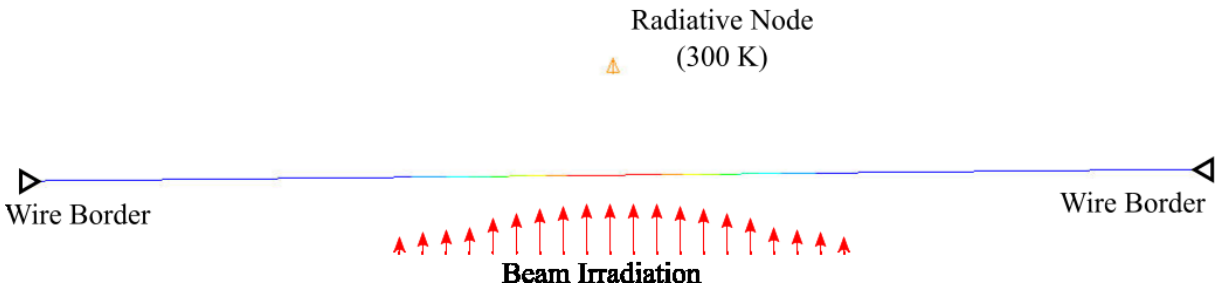

Figure 5: Scheme showing the main components of the wires 1D FEM model.

3. Results

3.1. Wire Temperature

In this section we calculate the temperature in the grid wire during operation. We study the two different scenarios: horizontal and vertical slit collimation with horizontal and vertical grid wire positions.

In Figure 6 we show the temperature evolution in the wire and in Figure 7 we show the temperature profile in the wire. We observe how for horizontal beam collimation the maximum temperature is <700 K, while in the case of a vertical slit, the beam size in the grid is much smaller and higher temperatures are attained, up to ~1400 K.

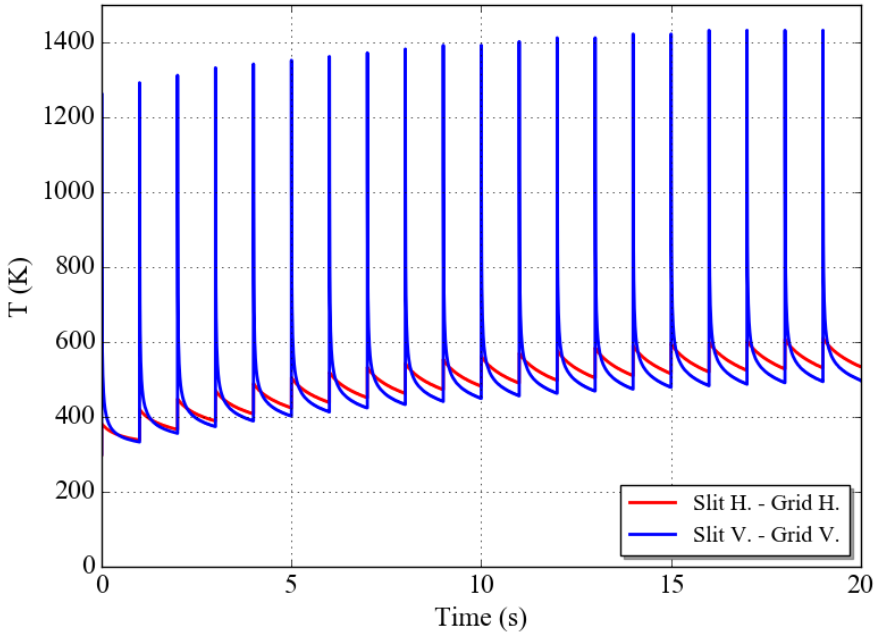

Figure 6: Temperature evolution for a tungsten wire in the grid with beam collimation with a horizontal slit of 100 μm. The analytical (blue) and FEM (red) models are shown.

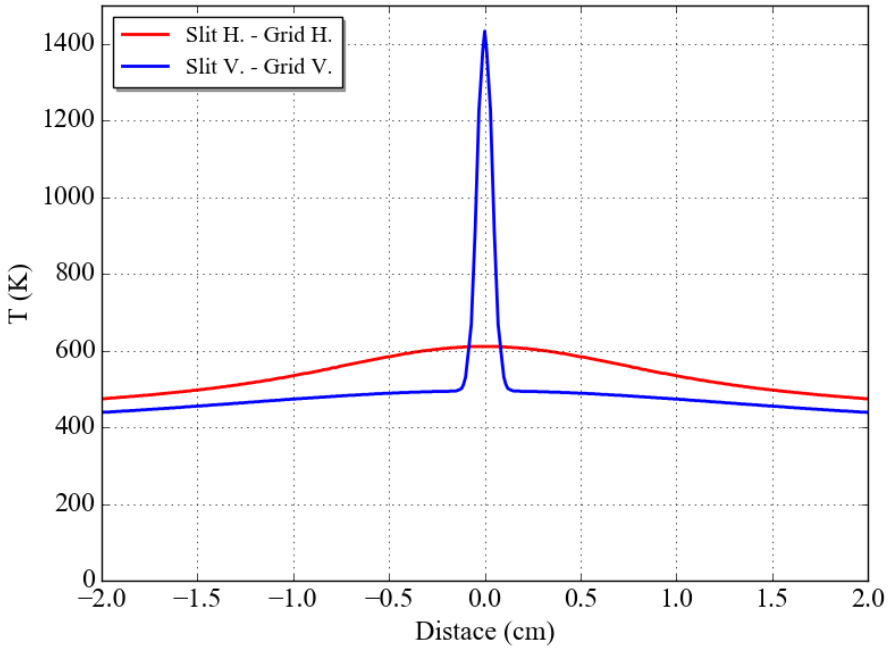

Figure 7: Temperature profile along the wire after the irradiation pulse in the grid position, with beam collimation with a horizontal (red) and a vertical (blue) slit of 100 μm.

3.2. **Mechanical Effects**

Regarding mechanical behaviour, in order to compensate thermal expansion, an initial preload will be applied to the wire. Therefore, before the pulse arrival, the wire will be in a tensile state. During the pulse, thermal expansion will reduce the tensile stresses in the wire or will bend the wire depending on the preload. If the preload is higher than the thermal expansion, the wire will keep its tensile condition. On the contrary, if the preload is lower than the thermal expansion, the wire will bend leading to transverse deformation.

If the preload is lost during operation, axial deformations will appear (ΔL). This deformation will bend the wire leading to transverse deformations (Δy). Using trigonometry we can calculate the transversal deformation Δy, see Figure 8 and Eq. (3)

$$\Delta y = \frac{\sqrt{2 \cdot \Delta L \cdot L + \Delta L^2}}{2} \qquad (3)$$

Therefore, in order to avoid wire bending, we need to guarantee operation in a tensile state. This means that the wire preload has to be higher than the force induced by thermal expansion.

In Table 3 the main operational conditions on the wires of the grid are shown. We observe that forces of ~0.4 N are expected. In order to compensate this thermal expansion, preloads of at least 40 g would be required.

For a nominal length of L=76 mm and an axial deformation ΔL~80 μm (see Table 3), a transversal deformation of Δy~1.7 mm appears. Therefore, even small axial deformation can lead to large transversal

errors. It is important to guarantee that the wire keeps its tensile stress conditions at any point of operation.

In order to guarantee a safety margin, preloads of ~100 g could be applied, which would mean a stress variation of ~1 GPa. The wire strength should be assessed and in order to avoid fatigue appearance due to cyclic loading, it is recommended to design the tungsten wire to operate with stresses below 50% of the tensile strength.

Table 3: Temperature, force and deformation for the Grid with beam collimation with a horizontal slit of 100 μm. Table shows estimations with the analytical and FEM models.

Case	T_{steady} **(K)**	T_{peak} **(K)**	F **(N)**	$\Delta\sigma$ **(MPa)**	ΔL **(μm)**
Slit H. - Grid H.	535	611	0.35	409	81
Slit V. - Grid V.	498	1433	0.25	292	65

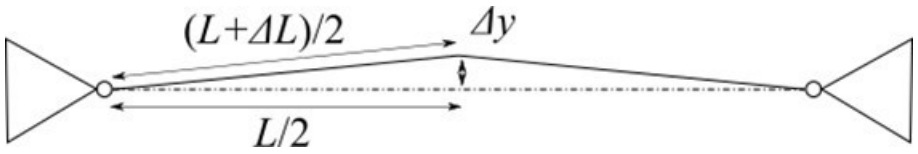

Figure 8: Deformed wire, where L is the original distance, ΔL the length increase, and Δy the transversal deformation.

4. **Conclusions**

We have studied the maximum temperatures, thermal force, and possible deformation for tungsten wires in the EMU/Grid.

In the tungsten wires of the EMU/Grid, temperatures are up to ~1400 K will be attained. This temperatures are below 1500 K that is the limit for operation with no thermionic emission. It is important to point out that the EMU/Grid can only be used jointly with the EMU/Slit. If the EMU/Slit is not previously inserted, the tungsten wires of the EMU/Grid could be seriously damaged.

We have assessed the thermal expansion and we conclude that a preload of at least 40 g (0.4N) needs to be effectively applied. In general, it is important to guarantee that the preload guarantees the tensile condition, and the wire does not get loose during operation. If the wire loses its tensile condition, large transversal deformation are expected, on the order of mm.

Appendix A: Material Properties

In this model we use tungsten material properties obtained from Linac 4 Cern Group, and reported in Refs. [8].

For the tungsten filament we take an emissivity of ϵ=0.1 [9]. This value is taken as a conservative estimation, other reported values point to emissivities for tungsten filament ~0.3 [10].

The material properties of the materials used in the work are summarized in Table 4.

Table 4: Material properties for tungsten [8].

Mat. Limit	**Tungsten**
Max. Temp. (K)	3673
Young Modulus (GPa)	405
Poisson Coefficient	0.3
Thermal Conductivity at 300 K (W m^{-1} K^{-1})	173
Density at 300 K (kg m^{-3})	19000
Specific Heat at 300 K (J kg^{-1} K)	133
Coefficient Of thermal expansion at 300 K (μm/m)	5

Appendix B: Measured Signal

The signal in the grid wires corresponds of the sum of the secondary electron emission from inlet (Y_e) and outlet ($Y_s \cdot \eta$) protons plus the charge of the deposited protons (1-η) [2, 11]:

$$Q = Y_e + Y_s \cdot \eta + (1 - \eta) \quad (4)$$

The secondary electron yield (Y) can be estimated as [2, 11]:

$$Y = \frac{P \cdot \frac{dE}{dx} \cdot dx}{E} \quad (5)$$

Where Y is the secondary electron production, dE/dx is the stopping power in the irradiated surface, dx is the surface depth for secondary electron production, typically 1 nm [2, 11] and E is the deposited energy per collision, typically 25 eV [2, 11]. P is the probability of an electron scaping which can be taken as ~0.5 [2, 11]. From Eq. (5) an estimation of the SEY can be obtained, however this value is subjected to a great incertitude, since it may change up to ~50% when the wire is exposed to the beam [11].

For tungsten irradiated with 3.63 MeV beams, the stopping power is ~600-1500 MeV/cm and Q of ~3 are expected [2].

The measured current in the Grid wires (I_{signal}) is the beam current that irradiates the wire (I_{wire}) by the charge multiplication (Q~3):

$$I_{signal} = Q \cdot I_{wire} \sim 3 \cdot I_{wire} \quad (6)$$

The current that irradiates the wire (I_{wire}) can be calculated for horizontal and vertical wires as:

$$I_{Wire\,H} = \frac{I^*}{2\pi\sigma_x\sigma_y}\int_{-\infty}^{\infty} e^{-\frac{x^2}{2\sigma_x^2}}\,dx \cdot \int_{-\frac{d}{2}}^{\frac{d}{2}} e^{-\frac{y^2}{2\sigma_y^2}}\,dy \approx \frac{I^*}{2\pi\sigma_x\sigma_y} \cdot \sqrt{2\pi} \cdot \sigma_x \cdot d = \frac{I^*}{\sqrt{2\pi}\sigma_y} \cdot d \quad (7)$$

$$I_{Wire\,V} = \frac{I^*}{2\pi\sigma_x\sigma_y}\int_{-d/2}^{d/2} e^{-\frac{x^2}{2\sigma_x^2}}\,dx \cdot \int_{-\infty}^{\infty} e^{-\frac{y^2}{2\sigma_y^2}}\,dy \approx \frac{I^*}{2\pi\sigma_x\sigma_y} \cdot \sqrt{2\pi} \cdot \sigma_y \cdot d = \frac{I^*}{\sqrt{2\pi}\sigma_x} \cdot d \quad (8)$$

Where I_{wire} is the beam intensity that irradiates the wire, I^* is the total beam intensity in the grid position, σ_x, σ_y the beam size and d the wire diameter.

The estimated signal values for the different configuration of the EMU, with horizontal and vertical slits and grids are shown in Table 5. The values for the expected signal are ~60 μA, which fells in the range of the electronics design 100 nA – 200 μA.

Table 5: Beam intensity in the grid (I^*), wire beam irradiation intensity (I_{wire}) and measured signal (I_{signal}) for different EMU configurations. The estimation is done for tungsten wires of 33 μm of diameter irradiated with a proton beam of 3.63 MeV.

Case	I^* **(mA)**	I_{wire} **(μA)**	I_{signal} **(μA)**
Slit H. Grid H.	0.56	21.1	63.2
Slit V. Grid V.		19.5	58.4

References

[1] Z. Izaola, “Emittance Unit Meter: Preliminary Design Review,” Jul-2016.

[2] B. Cheymol and R. Miyamoto, “Preliminary design of the ESS slit and grid system,” Internal ESS ESS-0020535-V1.1, juillet 2015.

[3] M. Munoz, M. Eshraqi, A. Jansson, S. Molloy, and M. Lindroos, “Description of Modes for ESS Accelerator Operation,” Internal ESS ESS-0038258 Rev. 3 Prelminary State, Nov. 2015.

[4] D. B. Pelowitz, “MCNPX user’s Manual Version 2.7.0,” LA-CP-11-00438, Apr. 2011.

[5] J. F. Ziegler, M. D. Ziegler, and J. P. Biersack, “SRIM – The stopping and range of ions in matter (2010),” *Nucl. Instrum. Methods Phys. Res. Sect. B Beam Interact. Mater. At.*, vol. 268, no. 11–12, pp. 1818–1823, Jun. 2010.

[6] C. Suplee, “Stopping-Power & Range Tables for Electrons, Protons, and Helium Ions,” *NIST*, 07-Oct-2009. https://www.nist.gov/pml/stopping-power-range-tables-electrons-protons-and-helium-ions.

[7] “ANSYS - Simulation Driven Product Development,” 04-Apr-2013. http://www.ansys.com/.

[8] T. Mora, I. Bustinduy, and F. Sordo, “ESS-Bilbao Beam Stoppers criteria (MEBT-BI-FC04-02),” 16-May-2016.

[9] B. Cheymol, “Effects of Energy Deposition Models and Conductive Cooling on Wire Scanner Thermal Load, Analytical and Finite Element Analysis Approach,” in *57th ICFA Advanced Beam Dynamics Workshop on High-Intensity and High-Brightness Hadron Beams (HB’16), Malmö, Sweden, July 3-8, 2016*, 2016, pp. 221–225.

[10] Mikron Instrument Company, “Table of emissivity of various surfaces.” .

[11] M. Plum, W. Christensen, R. Meyer, and C. Rose, “SNS Linac Wire Scanner System: Signal Levels and Accuracy,” *Proc. LINAC 2002 Gyeongju South Korea*, 2002.